ICSV13 - Vienna
The Thirteenth International Congress on Sound and Vibration
Vienna, Austria, July 2-6, 2006

COMPUTATION OF FLOW-INDUCED SOUND BY TURBULENT BOUNDARY LAYER USING LES METHOD

Huai-xin Zhang *[1], and Yu-cun Pan[1]

[1] School of Naval Architecture, Ocean and Civil Engineering, Shanghai Jiao Tong University
1954 Huashan Road, Shanghai,200030, China
hxzhang@sjtu.edu.cn (e-mail address of lead author)

Abstract
Large Eddy Simulation (LES) was used to investigate space-time field of the low Mach number, fully developed turbulent boundary layer on a smooth, rigid flat plate. The flowfield simulated by LES was taken as near-field sound sources and radiated sound from turbulent boundary layer (TBL) was studied using Lighthill's acoustics analogy. The radiated sound of dipole type, of quadrupole type, and of the sum of the two above were discussed. Comparing their power spectral densities, we concluded that in low Mach number, the wall shear stress (dipole type of source) was the predominant factor responsible for sound radiation from TBL.

INTRODUCTION

In classical acoustic problems, the sound wave was induced by the mechanical vibration of particular object. The fluid was only the medium of acoustic wave propagation. However, the objective of this study is to investigate the sound induced by the turbulence of fluid medium itself. The mechanism of hydrodynamic noise generation by turbulent flow has been a very interesting subject for fluid researches since Lighthill [1] laid the foundations to a general theory.

In this paper, the sound radiated from the low Mach number, fully developed turbulent boundary layer on a smooth, rigid flat plate is computed. The Lighthill's acoustic analogy method was used to investigate the hydrodynamic noise radiation. Lighthill pointed out that, in a low Mach number turbulent flow, the acoustic and turbulent fields are only weakly coupled so that the turbulent fluctuations, which are not influenced by the acoustic disturbances, act as sources of sound. In this study, the hybrid approach is used, in which the hydrodynamic and acoustic fields are decoupled. In the near-field, the hydrodynamic velocity and pressure are computed, which describe the nonlinear process of sound generation. The hydrodynamic terms as the sound source are used to calculate the far-field acoustic field, which describe the linear propagation of sound wave. Ffowcs Williams [2] pointed out that for sound generated by low Mach number flow, the influence of compressible could be neglected. So, in computation of fluid in near field, we can investigate it based on the equation of incompressible flow.

In this study, we should obtain the hydrodynamic terms of turbulent fluctuations, so, the Reynolds-averaged Navier-Stokes equations (RANS) method couldn't be used here, in which the governing equations are time-averaged. The direct numerical simulations (DNS) can provide the most precise, detailed fluctuating information, but the present computational resource can't support it to simulate high Reynolds- numbers flow. The information obtained by Large Eddy Simulation (LES) is no as exact as that obtained by DNS, but it can also reveal the elementary mechanism of turbulent flow. Moreover, the computational cost of a LES is much lower than that of a DNS. So, LES method was used in this study.

The paper was divided into essentially two sections. In Sec 1. the unsteady incompressible Navier-stokes equations were solved numerically using LES method to give an approximate description of the space-time field of the low Mach number, fully developed turbulent boundary layer on a smooth, rigid flat plate; In Sec 2. the far-field radiation of sound was calculated based on Curle's expansion [3] to the Lighthill acoustic analogy.

1. NUMERICAL SIMULATION OF TURBULENT BOUNDARY LAYER

Based on the theory of LES, the filtering operation was applied to the Navier-Stokes equations, and the Smagorinsky's model was chosen to parameterize the subgrid scale (SGS) stresses. In order to account for low-Reynolds-number SGS turbulence near the wall, the Van Driest exponential damping function was applied to the eddy viscosity ν_t, so that it could be damped to zero at the wall. The computation result shows the space-time field of fluctuating turbulent fluid motion near the wall. The more detailed computation process and result can be seen in Ref [4].

2. FLOW-INDUCED NOISE

2.1 Lighthill's acoustic analogy

The density fluctuation due to acoustic wave propagation from the hydrodynamic source region is governed by the convected wave equation:

$$\left[\left(\frac{\partial}{\partial t}+U_\infty\frac{\partial}{\partial x_1}\right)^2-c_0^2\frac{\partial^2}{\partial x_j\partial x_j}\right]\rho'=\frac{\partial^2 T_{ij}}{\partial x_i\partial x_j} \qquad (1)$$

Where, $\rho' = \rho - \rho_\infty$ is the density fluctuation, ρ_∞ is the free-stream density, c_0 is the sound speed in water at undisturbed conditions. We assume the free-stream velocity is U_∞, and $T_{ij} = \rho v_i v_j + \delta_{ij}[p - c_0^2(\rho - \rho_\infty)] - \tau_{ij}$ is the Lighthill stress tensor defined in terms of the fluctuating velocity relative to the free-stream value, $v_i = u_i - U_\infty \delta_{i1}$. In above equation, the usual summation convention applies for repeated subscripts, δ_{ij} is the Kronecker delta; and $\tau_{ij} = \mu(\frac{\partial v_i}{\partial x_j} + \frac{\partial v_j}{\partial x_i} - \frac{2}{3}\delta_{ij}\frac{\partial v_k}{\partial x_k})$ is the viscous part of Stokes stress tensor. Strictly speaking, it is almost impossible to resolve the equation (1) exactly. The hydrodynamic and acoustic terms are coupled each other, flow can induce sound and sound can be scattered by flow. To get the source item on the right-hand side of equation (1), the nonlinear equation should be solved strictly, which was a hard work. In order to study complex engineering applications, we should make some simplifying assumptions: in low Mach number flow, the two-way coupling is neglected, that is, the acoustic terms don't affect the hydrodynamic terms. Thus, we can consider the source terms on the right-hand side of equation (1) only contain the influence of flow to noise and the source terms can be obtained from the flow field.

If solid body exists in the sound source region ($T_{ij} \neq 0$) and the sound is generated by the solid surfaces, Curle [3] derived a simple solution for noise produced by the rigid surface moving through a quiescent medium.

$$\rho(\vec{x},t) - \rho_\infty = -\frac{1}{4\pi c_0^2}\left(\frac{\partial}{\partial x_i}\int_S \frac{n_j p_{ij}(\vec{y}, t - |\vec{r}|/c_0)}{|\vec{r}|} d^2 y - \frac{\partial^2}{\partial x_i x_j}\int_V \frac{T_{ij}(\vec{y}, t - |\vec{r}|/c_0)}{|\vec{r}|} d^3 y\right) \quad (2)$$

where $\vec{x}$ and $\vec{y}$ represent the position vectors of the observer and the sound sources, respectively, $r = |\vec{r}| = |\vec{x} - \vec{y}|$; $|\vec{r}|/c_0$ is called the delay time and represents the time interval of sound wave traveling from the sound sources to the observer. In the preceding equation $p_{ij} = p\delta_{ij} - \tau_{ij}$ and n_j is the directional cosine of the outward normal (into the fluid) to the rigid surface S over which the surface integration take place. The volume integral is taken over the entire unsteady flow region V external to the body. In the acoustic far field defined by $|\vec{r}| >> l_e / M$, where l_e is the typical eddy size, $M = U_\infty / c_0$ is the freestream Mach number, equation (2) simplifies to a form most suitable for numerical evaluation.

$$\rho(\vec{x},t) - \rho_\infty \approx \frac{1}{4\pi c_0^3}\frac{\partial}{\partial t}\int_S \frac{r_i}{|\vec{r}|^2} n_j p_{ij}(\vec{y}, t - \frac{|\vec{r}|}{c_0}) d^2 y + \frac{1}{4\pi c_0^4}\frac{\partial^2}{\partial t^2}\int_V \frac{r_i r_j}{|\vec{r}|^3} T_{ij}(\vec{y}, t - \frac{|\vec{r}|}{c_0}) d^3 y \quad (3)$$

In this computation, all coordinate variables, velocity components, and pressure are non-dimensionalized by the a characteristic length L, and the free-stream velocity U_∞ and $\rho_\infty U_\infty^2$, respectively. The time t is normalized by L/U_∞. Equation (3) can be rewritten as

$$\rho(\vec{x},t) - 1 \approx \frac{M^3}{4\pi}\frac{\partial}{\partial t}\int_S \frac{r_i}{|\vec{r}|^2} n_j p_{ij}(\vec{y}, t - M|\vec{r}|) d^2 y + \frac{M^4}{4\pi}\frac{\partial^2}{\partial t^2}\int_V \frac{r_i r_j}{|\vec{r}|^3} T_{ij}(\vec{y}, t - M|\vec{r}|) d^3 y \quad (4)$$

Furthermore, if both the body and the unsteady flow region are small compared with the typical acoustic wavelength l_e/M , the source region is acoustically compact. The far-field density can be approximated by

$$\rho(\vec{x},t)-1=\frac{M^3}{4\pi}\frac{x_i}{x^2}\dot{D}_i(t-M\left|x\right|)\ +\frac{M^4}{4\pi}\frac{x_ix_j}{x^3}\ddot{Q}_{ij}(\text{t-}M\left|x\right|) \tag{5}$$

where

$$\dot{D}_i(t)=\frac{\partial}{\partial t}\int_S n_jP_{ij}(\vec{y},t)d^2y \quad , \quad \ddot{Q}_{ij}(t)=\frac{\partial^2}{\partial t^2}\int_V T_{ij}(\vec{y},t)d^3y \tag{6}$$

In equation (5), there are two kinds of sound source: dipole source $\dot{D}_i$ and quadrupole source $\ddot{Q}_{ij}$, which respectively represent the compact surface and volume sound radiation. The pressure fluctuations and viscous shear tensors on the wall boundary generate sound radiation of dipole type; the Lighthill stress tensors behave as quadrupole.

2.2 computational result

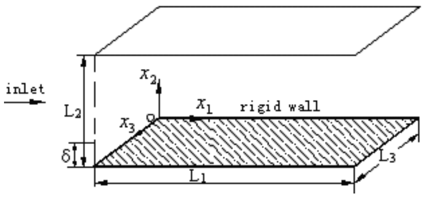

Figure 1. Computational domain of the turbulent boundary layer.

Figure 1 shows the computational domain of the turbulent boundary layer. To predict the far-field sound radiation, we assume there are symmetrical flow field at the both side of the flat plate. And the center of the plate was chosen to be the origin of coordinates, the vector of the observation point is chosen to be (2m,5m,2m). In this study, the lengths of three directions of computational box are chosen to be: ($8\delta \times 2\delta \times 8\delta$) ($\delta$ =0.0242658). The time-advanced step is chosen to be $\delta/5000u_\tau$. To satisfy the sampling precision and the resolution, the computation continued for 50000 steps after the time-averaged statistics had converged. The Reynolds number is set at $\mathrm{Re}=u_\tau\delta/\nu=800$, where u_τ is the wall shear velocity, δ is the thickness of the boundary layer. The Mach number $M=U_\infty/c_0$ =0.00054947 (the sound speed c_0=1500m/s)

There are three components of dipole source: $\dot{D}_1$、$\dot{D}_2$、$\dot{D}_3$. According to the assumption of symmetrical flow field on both side of the flat plate, we can deduce that the $\dot{D}_2=0$. There are nine components of quadrupole source: $\ddot{Q}_{11}$, $\ddot{Q}_{12}$, $\ddot{Q}_{21}$, $\ddot{Q}_{13}$, $\ddot{Q}_{31}$, $\ddot{Q}_{22}$, $\ddot{Q}_{23}$, $\ddot{Q}_{32}$, $\ddot{Q}_{33}$, in which three pairs are symmetrical: $\ddot{Q}_{12}$ and $\ddot{Q}_{21}$, $\ddot{Q}_{13}$ and $\ddot{Q}_{31}$, $\ddot{Q}_{23}$ and $\ddot{Q}_{32}$. So, only six quadrupole terms should be solved respectively.

Figure 2 shows the variation of quadrupole sources. we can find the amplitudes of the quadrupole $\ddot{Q}_{11}$、$\ddot{Q}_{22}$、$\ddot{Q}_{33}$ are relatively larger, and $\ddot{Q}_{11}$ is the largest, which shows the Lighthill stress tensor in streamwise is largest. In figure 3, the variation of dipole sources $\dot{D}_1$ 、 $\dot{D}_3$ was shown. To observe the variation of quadrupole and dipole source in frequency domain, Figure 4 shows the auto-power spectral density of quadrupole sources, Figure 5 shows the auto-power spectral density of dipole sources.

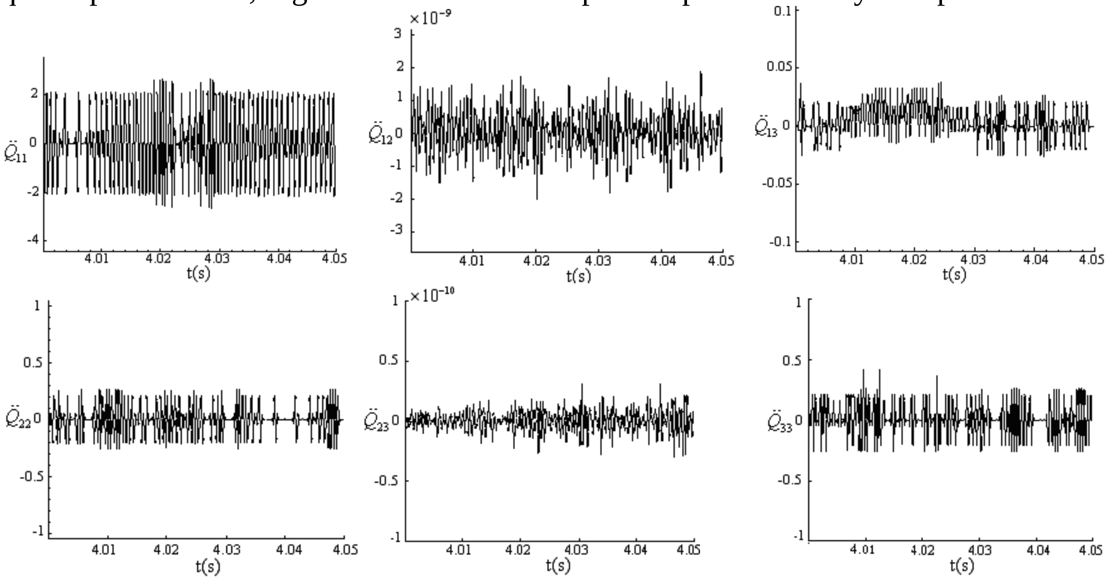

Figure 2. Variation of quadrupole

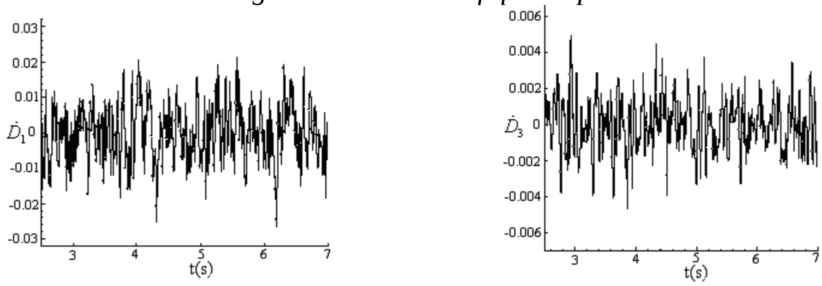

Figure 3. Variation of dipole

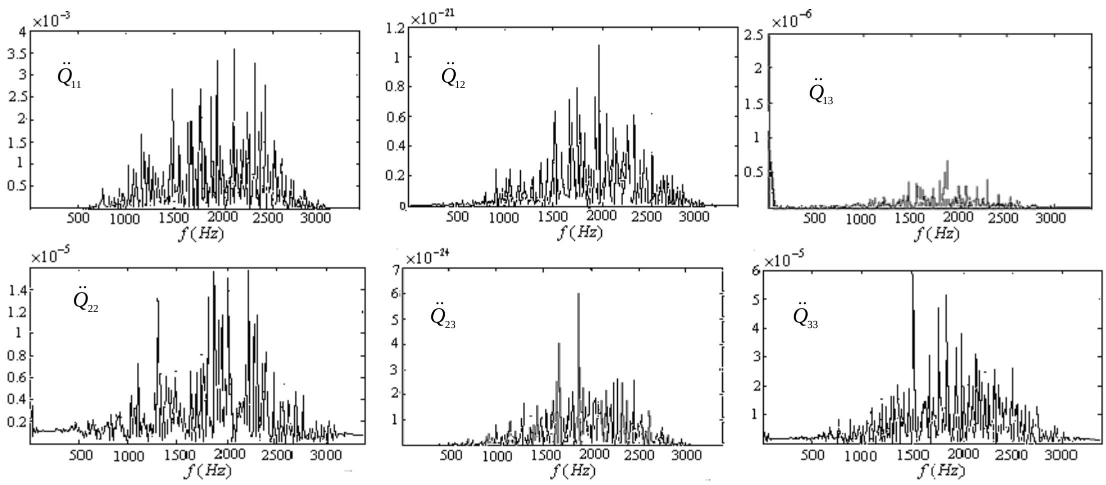

Figure 4. Power spectral density of quadrupole source

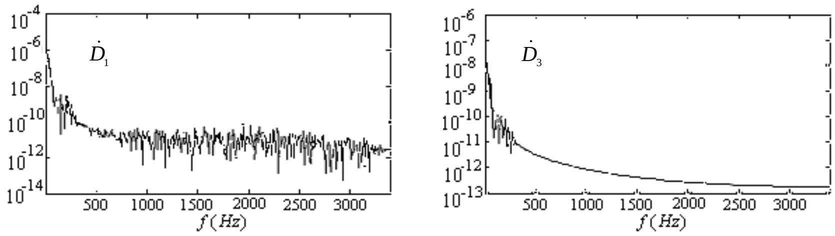

Figure 5. Power spectral density of dipole source

In the above figures, we can find the frequency of quadrupole fluctuations is relatively higher. All the quadrupole sources except $\ddot{Q}_{13}$ concentrate their energy in range of 1200～2500Hz. The frequency of dipole fluctuations is relatively lower, and the energy is concentrated in the domain of low frequency (under 500Hz). The reason may be that the dipole fluctuations were mainly caused by the fluctuations of viscous shear stress near the wall. As we known, in the vicinity of the walls, the high-speed fluid elements correspond to the sweep event toward wall; the low-speed fluid elements are generally being ejected from the wall regions. The viscous shear stress was intensively affected by the sweep and ejection events, and these events have low frequency and large amplitude value. So, the dipole source fluctuation was mainly in low frequencies. And the quadrupole sources associated with the second-order time derivative of Lighthill stress tensor. The Lighthill stress $T_{ij}^{'} \approx \rho u_i^{'} u_j^{'}$ is the product of velocities of different directions. The frequency velocity of fluctuations is relatively high, thus, the fluctuation of quadrupole source was in the domain of high frequencies.

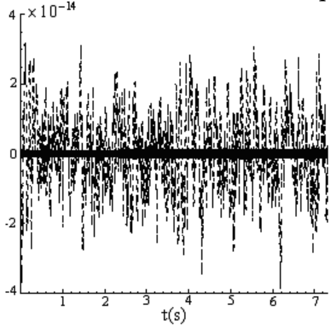

Fig6 variation of acoustic density at the far-field due to the quadrupole ——— and dipole− − −

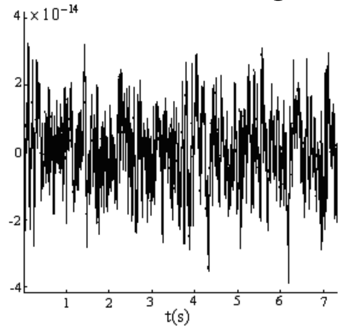

Fig7 variation of acoustic density at the far-field (summation of Quadrupole and dipole)

From Figure 4 to Figure 5, the sum of dipole $\dot{D}_i$ is smaller than the sum of quadrupole $\ddot{Q}_{ij}$. But according to the equation (5), acoustic densities due to the contribution of quadrupole sources at far-field is proportional to the fourth power of the Mach number, whereas that due to the contribution of dipole sources is proportional to the M^3. So, for the low Mach numbers, the contribution of the shear-stress dipole sources to the sound generation is larger than that of the quadrupole sources. In figure 6, the variation of acoustic density due to the contribution of dipole and quadrupole sources were shown respectively. Figure 7 shows the variation of acoustic density due to the contribution by the summation of dipole and quadrupole sources. From these figures, we can conclude that for Mach number $M = 0.00054947$, the turbulent shear-stress dipole sources dominates the whole acoustic field, and the contribution of quadrupole sources is almost negligible. It is observed that, the characteristic of acoustic field behaves as the characteristic of dipole sources.

According to the Lighthill analogy, the acoustic wave propagation was governed by a linear, inhomogeneous wave equation of a nearly incompressible fluid. So, we can obtain the relationship between acoustic pressure fluctuation p' and acoustic density fluctuation ρ' : $p' = p - p_\infty = c_0^2 \rho' = c_0^2(\rho - \rho_\infty)$. Thus, after we obtain the acoustic density fluctuation ρ' by Equation (5), we can research the variation of the acoustic pressure fluctuation p'. To observe the characteristic of acoustic pressure in frequency domain, we obtain the spectral density of it by Fourier transformation: $\phi_m(\omega) = \frac{1}{\pi}\int_{-\infty}^{\infty} R_{pp}(\tau) e^{-i\omega\tau} d\tau$ Where, $R_{pp}(\tau) = \left\langle p'(t) p'(t+\tau) \right\rangle$ is the auto-correlation function of acoustic pressure fluctuations.

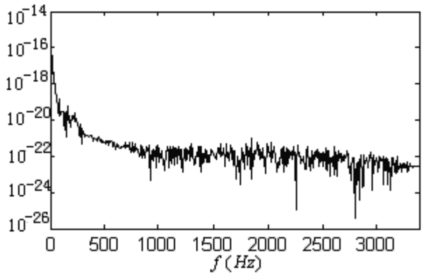

Figure 8 Power spectral density of sound pressure induced by dipole source

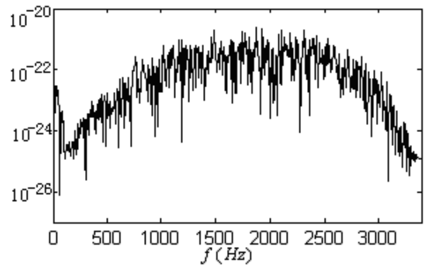

Figure 9 Power spectral density of sound pressure induced by quadrupole source

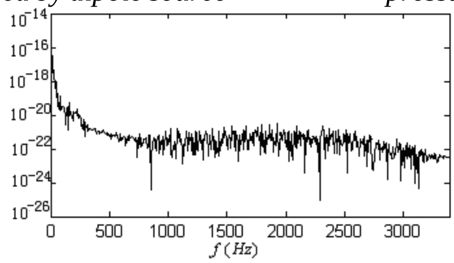

Figure 10 Power spectral density of sound pressure induced by the summation of dipole and quadrupole source

Figure 8 shows the power spectral density of sound pressure induced by dipole sources. For frequencies under 500Hz, the power spectral density drops sharply with increasing frequency. When the frequency is over 500Hz, the power spectral density tends toward calming and the amplitude of its fluctuation is small. So, the energy is concentrated in the domain of low frequencies. Figure 9 shows the power spectral density of sound pressure induced by quadrupole sources. For frequencies under 180Hz, the power spectral density drops with increasing frequency. When the frequency is over 180Hz, the power spectral density increases with increasing frequency and reaches its peak at 2300Hz. Over 2300Hz, the power spectral density drops again. So, the energy is concentrated in the domain between 1000 to 2500Hz. Figure 10 shows the power spectral density of sound pressure induced by the summation of dipole and quadrupole sources. This curve is very similar to that of the power spectral density of sound pressure induced by dipole sources in Figure 8. We can say that the sound pressure induced by dipole sources dominates the power spectral density of far-field sound radiation.

3. CONCLUSIONS

Large Eddy Simulation was used to investigate space-time field of the low Mach number, fully developed turbulent boundary layer on a smooth, rigid flat plate. The radiated sound from turbulent boundary layer was studied using Lighthill's acoustics analogy. It is observed that the energy of the computed far-field sound radiation is mainly concentrated in the domain of low frequency (under 500Hz). In addition, the sound level is so small that only precision instrument could measure it. Thus, It was difficult in laboratory to distinguish between the noise from TBL and the background noise. Numerical method would not introduce background noise and provide us a choice to resolve the problem.

There were many different assumptions about mechanism of acoustic sources in the turbulent boundary layer. Intensity of quadrupole sources associated with the fluctuation of Lighthill stress tensor, and intensity of dipole source depended on the fluctuation of wall shear stress. There are still debates between scholars about which is the predominant factor responsible for sound radiation from TBL [5],[6]: the dipole sources of wall shear stress fluctuations or the quadrupole source of turbulent Reynolds stress? In this study, the computational results show: for low Mach number, the power spectral of sound radiation induced by dipole source determines the power spectral of whole sound radiation. The dipole source dominates over the sound radiation field. The contribution of quadrupole source to the sound field can be neglected in some degree.

Acknowledgments

This work was supported by the national natural science foundation of China (No. 10372059). And the computations were carried out on the IBM P690 at the grid computing center of Shanghai Jiaotong University.

REFERENCES

[1]. Lighthill M J., "On sound generated aerodynamically II. Turbulence as a source of sound", Proc Royal Soc London, Ser A, **222**, 1-25(1954)

[2]. Ffowcs Williams J E, Hawkings D L., "Sound generation by Turbulence and surface in arbitrary motion", Phil.Trans.Roy.Soc., **264A**,321-342(1969)

[3].Curle N., "The influence of solid boundaries upon aerodynamic sound", Proc Royal Soc London, Ser A, **231,** 505-514(1955)

[4].Pan Yu-cun,Zhang Huai-xin.,"Investigation of wall pressure fluctuations beneath turbulent boundary layer by LES method", will be printed on Journal of ship Mechanics，2006

[5].Landahl M T. "Wave mechanics of boundary layer turbulent and noise", J.A.S.A, **57**(4), 824-831(1975)

[6].Hardin J C. Acoustic sources in the low Mach number turbulent boundary layer[J] . J.A.S.A., **90**(2): 1020-1031(1991)